Environmental Science & Technology

Article

pubs.acs.org/est

# Arsenate Accumulation, Distribution, and Toxicity Associated with Titanium Dioxide Nanoparticles in *Daphnia magna*

Mengting Li,[†,§] Zhuanxi Luo,[*,†,‡] Yameng Yan,[†] Zhenhong Wang,[†,‡] Qiaoqiao Chi,[†] Changzhou Yan,[*,†] and Baoshan Xing[‡]

[†]Key Laboratory of Urban Environment and Health, Institute of Urban Environment, Chinese Academy of Sciences, Xiamen 361021, China

[‡]Stockbridge School of Agriculture, University of Massachusetts, Amherst, Massachusetts 01003, United States

[§]University of Chinese Academy of Sciences, Beijing 100049, China

Supporting Information

**ABSTRACT:** Titanium dioxide nanoparticles (nano-$TiO_2$) are widely used in consumer products. Nano-$TiO_2$ dispersion could, however, interact with metals and modify their behavior and bioavailability in aquatic environments. In this study, we characterized and examined arsenate (As(V)) accumulation, distribution, and toxicity in *Daphnia magna* in the presence of nano-$TiO_2$. Nano-$TiO_2$ acts as a positive carrier, significantly facilitating *D. magna*'s ability to uptake As(V). As nano-$TiO_2$ concentrations increased from 2 to 20 mg-Ti/L, total *As* increased by a factor of 2.3 to 9.8 compared to the uptake from the dissolved phase. This is also supported by significant correlations between arsenic (*As*) and titanium (*Ti*) signal intensities at concentrations of 2.0 mg-Ti/L nano-$TiO_2$ ($R = 0.676$, $P < 0.01$) and 20.0 mg-Ti/L nano-$TiO_2$ ($R = 0.776$, $P < 0.01$), as determined by LA-ICP-MS. Even though *As* accumulation increased with increasing nano-$TiO_2$ concentrations in *D. magna*, As(V) toxicity associated with nano-$TiO_2$ exhibited a dual effect. Compared to the control, the increased *As* was mainly distributed in BDM (biologically detoxified metal), but *Ti* was mainly distributed in MSF (metal-sensitive fractions) with increasing nano-$TiO_2$ levels. Differences in subcellular distribution demonstrated that adsorbed As(V) carried by nano-$TiO_2$ could dissociate itself and be transported separately, which results in increased toxicity at higher nano-$TiO_2$ concentrations. Decreased As(V) toxicity associated with lower nano-$TiO_2$ concentrations results from unaffected *As* levels in MSFs (when compared to the control), where several *As* components continued to be adsorbed by nano-$TiO_2$. Therefore, more attention should be paid to the potential influence of nano-$TiO_2$ on bioavailability and toxicity of cocontaminants.

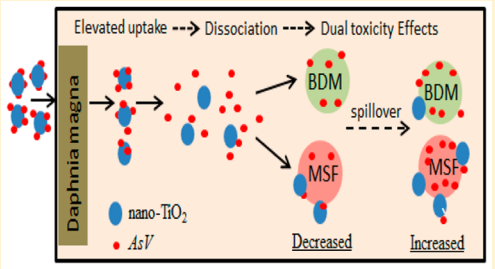


## 1. INTRODUCTION

Potential health hazards and environmental impacts of manufactured nanoparticles (MNPs) have become a significant concern with the rapid development of nanotechnology.[1−4] Some nanoparticles, such as nanosized titanium dioxide (nano-$TiO_2$), are used in a variety of consumer products, such as sunscreens, cosmetics, paints, and surface coatings[5] as well as in the environmental decontamination of air, soil, and water.[6,7] Such widespread use raises concern that nano-$TiO_2$ could pose a risk to both ecosystems and human health.[8−11]

Most previous studies on health risks and environmental impacts of nano-$TiO_2$ have focused on their biological effects and toxicity levels. Production of reactive oxygen species (ROS) and their subsequent inflammatory effects are considered the main mechanisms for nano-$TiO_2$ toxicity.[12−14] For aquatic organisms, several studies considered the effects of nano-$TiO_2$ on water fleas (*Daphnids magna*, *Daphnia pulex*, and *Ceriodaphnia dubia*), and 48-h EC50 were generally greater than 100 mg/L.[15−17] Additionally, nanoparticles can adsorb metals and organic contaminants due to their large surface areas;[18−20] nano-$TiO_2$ sorption behavior includes electrostatic forces and chemical bonding. It has been well established that nano-$TiO_2$ has the potential to facilitate the entry of cocontaminants adsorbed by nanoparticles into aquatic organisms and to subsequently promote potential toxic effects. A previous study demonstrated that when exposed to As(V)-contaminated water in the presence of nano-$TiO_2$, arsenic (*As*) concentrations in carp increased by 132% after 25 d exposure.[21] Another study stated that the presence of nano-$TiO_2$ increased cadmium (Cd) concentrations in carp by 146%, and that a positive correlation existed between Cd and nano-$TiO_2$ concentrations.[22] In a recent study, Yang et al.[23] found that nano-$TiO_2$ acted as a Cd bioaccumulation carrier for ciliate *Tetrahymena thermophila*. Hence, nano-$TiO_2$ can transport cocontaminants into aquatic organisms.

However, little available information describes the impact of nanoparticles on biokinetics of various cocontaminants in

Received: March 12, 2016
Revised: June 28, 2016
Accepted: August 2, 2016
Published: August 2, 2016





DOI: 10.1021/acs.est.6b01215
Environ. Sci. Technol. 2016, 50, 9636−9643

aquatic organisms, particularly for the spatial and subcellular distribution of cocontaminants associated with nanoparticles. Total bioaccumulation, measured as the whole-body metal content, is often a poor indicator of toxicity, which suggests that the manifestation of toxicity in these organisms can be the result of a site-specific accumulation in sensitive tissues.[24] Thus, "conventional" analytical methods (such as AAS, ICP-OES, and ICP-MS after whole-body sample digestion) are not well-suited as a means to gain further insight into how nanoparticles and cocontaminants affect aquatic organisms. This is because they only reveal whole-body concentrations and do not provide information related to tissue-specific elemental distribution. Laser ablation inductively coupled plasma mass spectrometry (LA-ICP-MS) is rapidly emerging as the method of choice in obtaining detailed and sensitive visualization of elemental distribution within biological samples.[25−28] The main advantages of LA-ICP-MS technologies are in their instrumentation accessibility, high sample throughput, their significantly lower rates of polyatomic ion formation, excellent detection limits (down to sub$\mu$g/g levels under optimum conditions), and a lateral resolution of only a few $\mu$m. Therefore, using mapping technologies with higher resolutions can help obtain valuable spatial distributions of cocontaminants associated with nanoparticles taken up by aquatic organisms as well as aid us in determining where nanoparticles transport cocontaminants and where they subsequently accumulate. However, spatial distribution of cocontaminants associated with nanoparticles has not been previously investigated.

It is also critical to understand internal processes of accumulated cocontaminants in the presence of nanoparticles. Subcellular partitioning of metals within aquatic invertebrates can reflect the internal processing during metal accumulation and provide valuable information concerning metal toxicity and tolerance.[29,30] Manifestations of sublethal toxicity can coincide with changes in subcellular partitioning, particularly in cases where saturation of certain metal detoxification systems take place.[31] Similarly, partitioning of metal conglomerates or metal-rich granules (MRG) and binding with inducible metal-binding proteins (metallothioneins, MT) can reveal metal detoxification, which has been linked to metal tolerance and resistance.[32] Subcellular distribution of nanoparticles with cocontaminants based on subcellular partitioning could aid in our understanding of internal processes related to the accumulation of cocontaminants and thus further our understanding of their combined toxicity.

The aims of this study were to quantify accumulation, spatial and subcellular distribution, and toxicity of arsenate (As(V)) associated with nano-$TiO_2$ owing to the high risk of potential *As* contamination on a global scale.[33] More importantly, there is presently little information available on accumulation and the subsequent spatial and subcellular distribution of As(V) associated with nano-$TiO_2$ as well as its toxicity in aquatic organisms. We used *Daphnia magna*, an ecologically important freshwater zooplankton, as the model organism. This study will better clarify potential hazards of manufactured nanoparticles as carriers of cocontaminants.

## 2. MATERIALS AND METHODS

**2.1. Preparation and Characteristics of Test Solutions.** We obtained uncoated, powdered nanoscale Degussa A100 $TiO_2$ (nano-$TiO_2$) nanoparticles (99.7%, anatase, CAS No. 1317-70-0) with an average surface area of 50 $m^2$ $g^{-1}$ and a particle size of 25 nm from Sigma-Aldrich Corporation (St. Louis, MO, USA). These A100 particles were composed of 100% anatase $TiO_2$. A stock solution of 1.0 g-Ti/L nano-$TiO_2$ was prepared by dispersing nanoparticles in ultrapure water (Millipore, Billerica, MA, USA) and applying sonication for 10 min (50 W $L^{-1}$ at 40 kHz), and a further 10 min application of sonication was conducted each day immediately before dosing. In addition, we observed nano-$TiO_2$ aggregate morphology in test solutions using a scanning electron microscope (SEM, S-4800, Hitachi, Japan). We then determined the average diameter and $\zeta$-potential of nano-$TiO_2$ by a dynamic light scattering device (DLS, Malvern Instruments Ltd., Malvern, UK). We used $Na_3AsO_4{\cdot}12H_2O$ to prepare arsenate stock solutions. A stock solution was made at a concentration of 100 mg/L. We stored stock solutions in the dark at 4 °C until usage.

For the adsorption experiments, we prepared all exposure media 1 h prior to use to allow As(V) adsorption on nano-$TiO_2$ to reach equilibrium. We did this by diluting the stock solution with the daphnia culture medium (SM7, containing only $CaCl_2$, $MgSO_4$, $K_2HPO_4$, $KH_2PO_4$, $NaNO_3$, $NaHCO_3$, $Na_2SiO_3$, $H_3BO_3$, and KCl without disodium ethylenediaminetetraacetic acid, trace metals, or vitamins) reconstituted according to the OECD guideline standard.[34]

**2.2. Arsenate Adsorption on Nano-$TiO_2$.** It is essential to understand *As* adsorption behavior on nano-$TiO_2$ in biokinetics. To study As(V) adsorption on nano-$TiO_2$, we prepared 2 and 20 mg-Ti/L (final concentration) nano-$TiO_2$ suspensions in a high-density polyethylene beaker containing 100 mL of SM7. As(V) was then added to nano-$TiO_2$ suspensions (1 $\mu$M As). We collected 1.5 mL of the nano-$TiO_2$ suspension at 0.5, 1, 2, and 3 h and centrifuged twice for 10 min at 12 000*g* using a high-speed centrifuge (from which 91.8% to 95.0% of nano-$TiO_2$ was removed). We then used 1 mL of the collected supernatant and 1 mL of the original nano-$TiO_2$ suspension to measure *As* concentrations. We subsequently calculated the As(V) percentage adsorbed on nano-$TiO_2$ ($n$ = 3).

**2.3. Test Organism.** We obtained *D. magna* from Sun Yat-sen University (Guangzhou, China) and continuously cultured the medium in our laboratory. We fed *Scenedesmus obliquus* to *D. magna* daily at a density of $10^5$ cells/mL, and we changed the water every 2 days. We maintained the culture at a constant temperature (22 °C ± 2 °C) under a natural light−dark cycle.

**2.4. Toxicity Experiment.** We conducted a 24 h long toxicity experiment based on the modified OECD standard procedure.[34] There were eight As(V) concentrations in total (0, 5, 10, 15, 20, 30, 40, and 50 $\mu$M) as well as three nano-$TiO_2$ levels (0.0, 2.0, and 20.0 mg-Ti/L) in the medium. We conducted As(V) and nano-$TiO_2$ toxicity experiments separately to serve as controls on assessing nano-$TiO_2$ effects on As(V) toxicity. For each treatment, we placed 10 neonates (from 6 to 24 h old) of similar size from a designated brood in a 50 mL glass beaker containing 30 mL of the test solution. We assessed the mortality of individuals in each container at the end of this experiment. Organisms that did not swim within a 15 s period of gentle agitation were considered deceased.[34] We conducted all experiments in triplicate. We calculated 24-h EC50 values as well as their associated 95% confidence intervals (95% CI) using a probability unit graphical method. We designated the no observed effect concentration (NOEC) value as the highest tested concentration when compared to the control with no statistically significant effects within the exposure period.


DOI: 10.1021/acs.est.6b01215
Environ. Sci. Technol. 2016, 50, 9636−9643

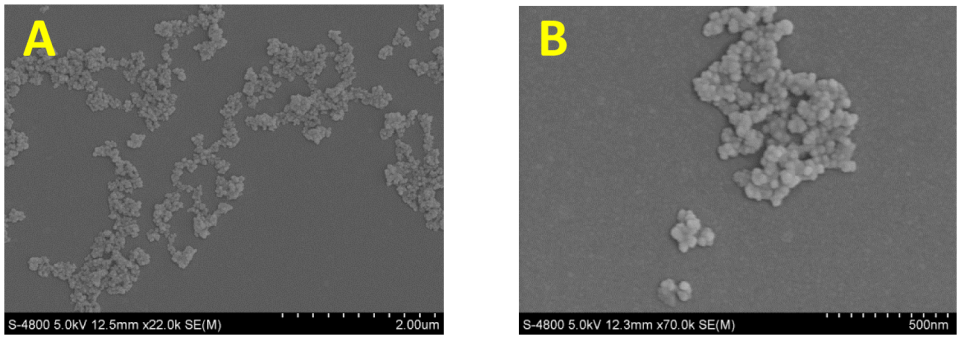


**Figure 1.** SEM images of nano-$TiO_2$ aggregates (20.0 mg-Ti/L) in culture medium (pH 8.0). Panels A and B were taken from the same sample, but panel B is at a higher magnification.

**2.5. Accumulation Experiments.** For accumulation experiments, we exposed *D. magna* to As(V) adsorbed in either low (2.0 mg-Ti/L) or high (20.0 mg-Ti/L) concentrations of nano-$TiO_2$ for 3 h. We prepared nano-$TiO_2$ test solutions along with three final levels of 0 (control), 2, and 20 mg-Ti/L in beakers by diluting the nano-$TiO_2$ stock. The final As(V) exposure concentration was also 1 $\mu$M. We employed three replicates for each treatment, each containing 200 7-day old daphnia specimens of similar size (1 individual/10 mL). We first removed daphnids and allowed them to evacuate their guts for 3 h in a SM7 medium without food particles present.[35] We used short-term exposure to measure the unidirectional influx under the assumption that the efflux was negligible during the initial exposure phase.[35] We collected 10 daphnids at 20, 40, 60, 90, 120, and 180 min from each of the three exposure beakers for arsenic and *Ti* content analysis. At 180 min, we collected 5 and 100 daphnids from each of the three exposure beakers for spatial and subcellular distribution analysis, respectively. We washed the collected daphnids for a few seconds in ultrapure water to remove the surrounding exposure medium, and then washed the samples in 5 mM $Na_2EDTA$ for 1 min to remove externally bound nanoparticles and aggregates. Then we used a 0.1 M potassium phosphate buffer (pH 7.0) to remove arsenic. After quickly washing in ultrapure water to remove the EDTA and potassium phosphate buffer, we put the daphnids samples into bullet vials.[36] Water samples were also collected at this point in time. For particle content (the body burden of arsenic and titanium in daphnia) analyses, sampled daphnia were treated following a modified method by Nathalie Adam et al.[36]

Briefly, after 50 $\mu$L of $HNO_3$ (69%) and (after 12 h) 50 $\mu$L of HF (40%) were added, daphnids were dissolved 4 h later by microwave digestion (4 min 100 W, 3 min 180 W, 2 min 180 W, 2 min 300 W, 2 min 300 W, 2 min 450 W), after which the samples were diluted to 1−2% $HNO_3$. We then used an Agilent 7500a ICP-MS to analyze *As* and *Ti*. Detailed procedures can be found in the Supporting Information section.

**2.6. Spatial Distribution Experiments.** We oven-dried the collected daphnids to a constant weight of 60 °C overnight. Laser sampling was conducted using a GeoLas 2005 system. We transported the laser-generated aerosol from the ablation cell to the ICP-MS instrument using a 1 m transfer tube with an internal diameter of 3 mm. The standard GeoLas 2005 ablation cell is a closed-cell design and basically consists of a cylindrical volume of approximately 40 $cm^3$. We placed an in-house sample mount in the cell, which reduces the effective cell volume to ∼14 $cm^3$. We used helium for its advantages as a carrier gas.[37,38] We used argon (*Ar*) as the makeup gas and mixed it with the carrier gas via a T-connector before exposure to inductively coupled plasma (ICP). We used an Agilent 7500a ICP-MS instrument to acquire ion-signal intensities. Detailed operating conditions for the laser and the ICP-MS instrument are provided in Table S1.

**2.7. Subcellular Distribution Experiments.** We determined subcellular partitioning of total *As* and *Ti* in *D. magna* body tissues using the methods of differential centrifugation described by Wang et al.[29] We obtained a total of five different fractions, including cellular debris (containing cell membranes), organelles (containing nuclear, mitochondrial, microsomes, and lysosomes), heat-denatured protein (HDP, containing enzymes), heat-stable protein (HSP, or metallothionein-like proteins), and metal-rich granules (MRG). We separately assayed all fractions for total *As* and *Ti* concentrations to allow us to estimate *As* and nano-$TiO_2$ subcellular partitioning. Results are expressed in mg (dry weight) per individual. The rate of recovery of the subcellular fraction was approximately 86% to 105%.

**2.8. Statistical Analysis.** We repeated all experiments independently on three separate occasions, and data were recorded as means with standard deviations (SD). We evaluated the homogeneity of variance, and used one-way analysis of variance (ANOVA) with a Tukey's range test to detect significant differences between control and treated groups. We utilized the Spearman's rank correlation coefficient test to determine correlations between *As* and *Ti* intensities in LA-ICP-MS maps. We considered $P < 0.05$ statistically significant for all data analysis.

## 3. RESULTS AND DISCUSSION

**3.1. Nano-$TiO_2$ Characterization and Arsenate Sorption.** Using SEM, we observed that nano-$TiO_2$ tended to aggregate with sizes from a few hundred nanometers (nm) to several micrometers ($\mu$m) in diameter in the SM7 medium (Figure 1). The average nano-$TiO_2$ diameter measured by DLS increased from approximately 250 to 600 nm with increasing concentrations of nano-$TiO_2$ from 2.0 to 20.0 mg-Ti/L in the SM7 medium. This indicated that the aggregate formation was concentration-dependent. According to UV−vis, with initial concentrations of 2.0, 10.0, and 20.0 mg-Ti/L, 60.0%, 52.0%, and 43.0% of $TiO_2$ nanoparticles remained in the daphnia media supernatant, respectively, after 24 h (SI, Figure S1), suggesting that any daphnia within the water column will be exposed to nanoparticulate aggregates for an extended period. Additionally, the size of nano-$TiO_2$ in media in the presence of As(V) significantly decreased and showed greater stabilization compared to the size of nano-$TiO_2$ in the absence of As(V). Specifically, when 0, 1, 10, and 100 $\mu$M As(V) was added to


DOI: 10.1021/acs.est.6b01215
Environ. Sci. Technol. 2016, 50, 9636−9643

20.0 mg-Ti/L of nano-$TiO_2$, average diameters of nano-$TiO_2$ were 600, 580, 530, and 470 nm, respectively. Consistent with the size decrease, the $\zeta$-potentials also dropped dramatically. When 0, 1, 10, and 100 $\mu$M As(V) was added to 20.0 mg-Ti/L of nano-$TiO_2$, the $\zeta$-potential of the solutions were $-0.71 \pm 0.05$, $-4.90 \pm 0.08$, $-15.20 \pm 0.52$, and $-29.70 \pm 1.21$ mV, respectively. We can infer that the electrostatic repulsion between nano-$TiO_2$ particles was enhanced because nano-$TiO_2$ and As(V) are both negatively charged. Therefore, after the addition of As(V), nano-$TiO_2$ suspension stability significantly increased, resulting in potential ecological accumulation of relative As(V) in *D. magna* within the water column.[39,40]

As(V) adsorption onto 2.0 and 20.0 mg-Ti/L nano-$TiO_2$ are provided in Figure 2. Adsorption occurred rapidly with

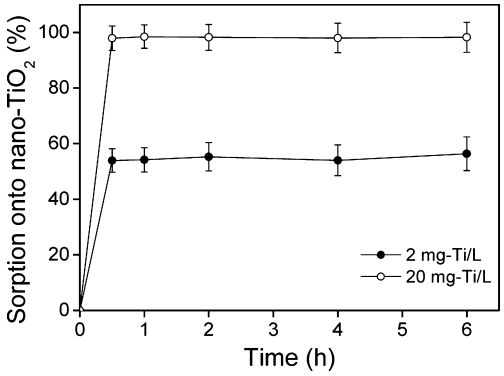


**Figure 2.** Adsorption of arsenate on nano-$TiO_2$. Values are means $\pm$ SD ($n$ = 3).

equilibrium occurring within the first 30 min. Additionally, more As(V) can be adsorbed with greater amounts of nano-$TiO_2$ (Figure 2). Specifically, 56.0% and 98.0% of As(V) (1 $\mu$M) can be adsorbed onto 2.0 and 20.0 mg-Ti/L nano-$TiO_2$, respectively (Figure 2).

**3.2. Arsenate Toxicity Associated with Nano-$TiO_2$.** Although other studies have investigated the toxic effects of As(V) or nano-$TiO_2$ on *D. magna*,[41,42] our study provides some of first published data on acute As(V) toxicity under the influence of nano-$TiO_2$. The median growth inhibition concentration (24-h EC50) of As(V) was 1.2 mg/L for *D. magna* in the absence of nano-$TiO_2$. No mortality was found in nano-$TiO_2$ concentrations less than 100 mg/L. For this reason, the contribution of bare nano-$TiO_2$ to mortality can be neglected in the following discussion. Despite that nano-$TiO_2$ had no observable toxic effects on *D. magna* at concentrations less than 20.0 mg-Ti/L, it may still have influence on the toxicity of As(V). To validate this hypothesis, we examined toxic effects of As(V) in the presence of nano-$TiO_2$. It is interesting to note that the addition of nano-$TiO_2$ had an unexpected dual effect on As(V) toxicity in *D. magna*. Namely, As(V) toxicity on *D. magna* first decreased at 2 mg-Ti/L nano-$TiO_2$ and then increased at 20 mg-Ti/L nano-$TiO_2$ (Figure S2). Compared to the control, 24-h As(V) EC50 of 1.68 mg/L increased by a factor of 1.4 in the presence of 2.0 mg-Ti/L nano-$TiO_2$, whereas 24-h As(V) EC50 of 0.72 mg/L decreased by 40.0% in the presence of 20.0 mg-Ti/L nano-$TiO_2$. At first, nano-$TiO_2$ reduced toxic effects of As(V) at a lower nano-$TiO_2$ concentration (2.0 mg-Ti/L). Rosenfeldt et al. reported that 48-h As(V) EC50 values increased by 32% in *D. magna* in the presence of 2.0 mg/L nano-$TiO_2$.[43] This result was consistent with ours at the lower nano-$TiO_2$ concentration. However, our results were in sharp contrast to Wang et al.,[44] who reported an increase in As(V) toxicity in *Ceriodaphnia dubia* in the presence of either lower or higher nano-$TiO_2$ concentrations (from 1 to 300 mg-Ti/L). The different model organisms used between the studies could be one potential explanation for this disparity.

**3.3. Arsenate Accumulation Associated with Nano-$TiO_2$ in *Daphnia magna*.** As(V) uptake by *D. magna* clearly increased with increasing nano-$TiO_2$ concentrations (Figure 3). After exposing *D. magna* to a series of nano-$TiO_2$ concentrations for 3 h, the dry-weight concentration factor (DCF) for total *As* and *Ti* increased ($P < 0.05$, $n = 3$), following a nonlinear pattern with apparent saturation, and uptake processes were biphasic (Figure 3). We observed a linear uptake of As(V) ($r^2$ = 0.98, 0.99, and 0.99) and nano-$TiO_2$ ($r^2$ = 0.97 and 0.98) within the first 80 min, but As(V) and nano-$TiO_2$ uptake apparently reached saturation after 80 min of exposure. As nano-$TiO_2$ concentrations increased from 2 to 20 mg-Ti/L, total *As* DCF increased by a factor of 2.3 to 9.8 compared to uptake during the dissolve phase (Figure 3a) after 3 h exposure. At the same time, equilibrium concentrations of *Ti* increased from 1.3 to 5.6 mg/g as initial concentrations of nano-$TiO_2$ increased from 2.0 to 20.0 mg-Ti/L.

Such increases in As(V) accumulation with increasing nano-$TiO_2$ concentrations could be attributed to nanoparticulate ingestion (Figure 3b). *Daphnia magna* were able to consume particles of 0.4−40 $\mu$m in size,[45,46] and nano-$TiO_2$ tended to aggregate and agglomerate in the exposure medium, which could easily be seized by *Daphnia magna*. It had also been reported that *D. magna* ingest bacteria of approximately 200 nm in size.[47] As nano-$TiO_2$ concentrations increased from 2.0 to 20.0 mg-Ti/L, the As(V) DCF increased by a factor of 2.3 to

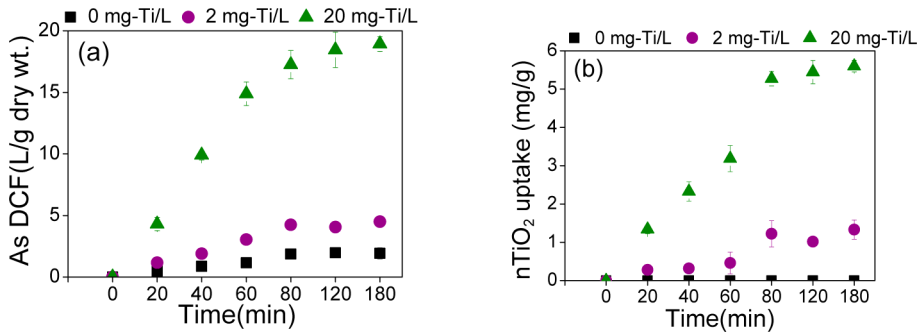


**Figure 3.** (a) Uptake of arsenate by *Daphnia magna* under different nano-$TiO_2$ concentrations (0.0, 2.0, and 20.0 mg-Ti/L). (b) Nano-$TiO_2$ accumulation in *Daphnia magna* at different concentrations during 3 h *Daphnia magna* exposure. Values are means $\pm$ SD ($n$ = 3).



DOI: 10.1021/acs.est.6b01215
Environ. Sci. Technol. 2016, 50, 9636−9643

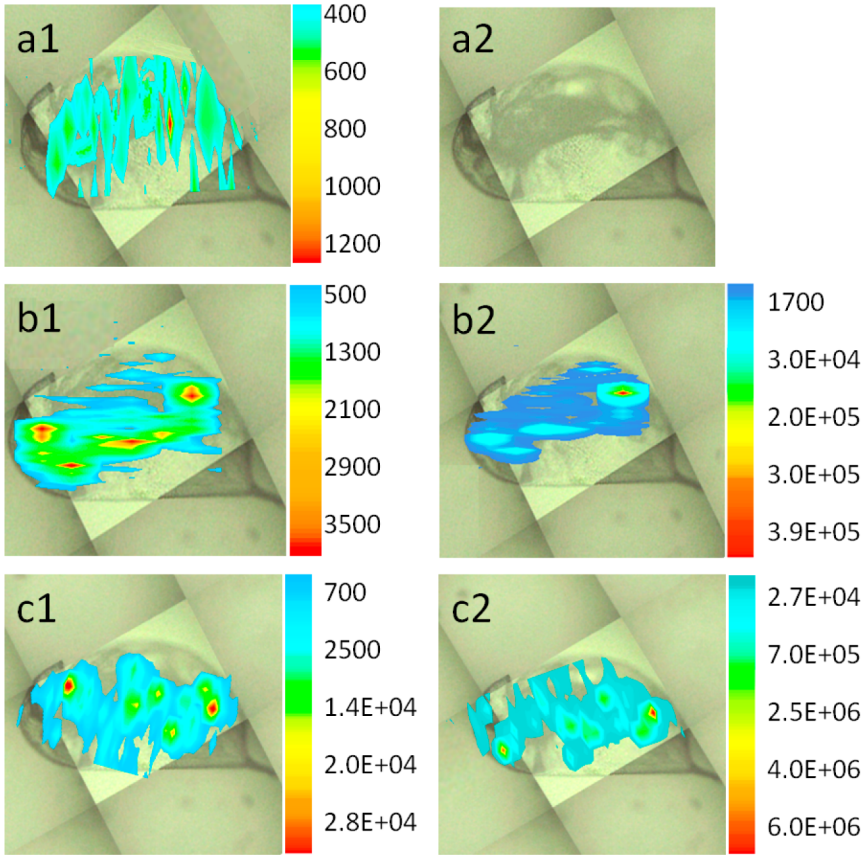


**Figure 4.** Arsenic mapping in *Daphnia magna* under different nano-$TiO_2$ concentrations (a1, b1, and c1 represent 0.0, 2.0, and 20.0 mg-Ti/L, respectively). Panels b2 and c2 are titanium mapping in *Daphnia magna* under different nano-$TiO_2$ concentrations (b2 and c2 represent 2.0 and 20.0 mg-Ti/L, respectively). Signals are shown as a gradient of intensity (CPS) with the corresponding photograph of *Daphnia magna*.

9.8 compared to uptake during the dissolved phase (Figure 3a) after 3 h exposure. Similar results were found in other studies. Fan et al., for example, determined that the existence of 2.0 mg-Ti/L nano-$TiO_2$ enhanced copper accumulation in *D. magna* from 18% to 31%.[48] Tan et al. observed that as nano-$TiO_2$ concentrations increased from 0.5 to 2.0 mg-Ti/L, the Cd DCF in *D. magna* increased by a factor of 11.0 to 16.9, and that zinc (Zn) increased by a factor of 37.2 to 51.3 compared to uptake from the dissolved phase.[35] This illustrates that the nano-$TiO_2$ carrying capacity for different metals differs. Moreover, the fact that uptake processes for As(V) and nano-$TiO_2$ were correlated showed that nano-$TiO_2$ could be a positive carrier in facilitating the accumulation of As(V) in *D. magna*. This was also supported by the significant correlation between As(V) and *Ti* intensities ($P < 0.01$) ascertained from LA-ICP-MS (see section 3.4). At the same time, correlation coefficients increased from 0.676 to 0.776 as nano-$TiO_2$ concentrations increased from 2.0 to 20.0 mg-Ti/L. This means that greater *As* concentrations were carried by nano-$TiO_2$ that accumulated in *D. magna* as nano-$TiO_2$ concentrations increased.[49]

**3.4. Spatial Distribution of Arsenic and Titanium in *Daphnia magna*.** *As* and *Ti* spatial distributions with their corresponding *D. magna* photographs are provided in Figure 4. Arsenic and *Ti* signals were more intense in the gut of the organism. Intensities of measured *As* in the gut were greater by a factor of 5 to 10 than in other tissues, with nano-$TiO_2$ concentrations increasing from 0.0 to 20.0 mg Ti/L ($P < 0.05$, $n = 3$). In the same way, intensities of measured *Ti* in the gut were greater by a factor of 40 and 95 than in the surrounding tissues at concentrations of 2.0 and 20.0 mg Ti/L nano-$TiO_2$ ($P < 0.05$, $n = 3$), respectively (Figure 4). There were also significant correlations between *As* and *Ti* intensities at nano-$TiO_2$ concentrations of 2.0 mg-Ti/L ($R = 0.676$, $P < 0.01$) and 20.0 mg-Ti/L ($R = 0.776$, $P < 0.01$).

Previous studies proposed that the dissociation of metals from colloidal organic matter was the result of the critical process of metal internalization. It is therefore possible that metals sorbed on nano-$TiO_2$ were dissociated in the gut of daphnids, and free metal ions were bound to specific protein transporters.[50,51] In our study, almost all As(V) associated with nano-$TiO_2$ accumulated in the gut of *D. magna*, which was ascertained by As(V) and *Ti* intensities from LA-ICP-MS. Due to changes in pH levels in the gut of organisms, it is conceivable that As(V) could dissociate itself from nano-$TiO_2$, especially under reversible physical sorption through electrostatic forces.[51,52] This is also demonstrated by our results in subcellular distribution (see section 3.5).

**3.5. Subcellular Distribution of Arsenic and Titanium in *Daphnia magna*.** Subcellular concentrations of *As* and *Ti* in the five subcellular fractions (including metal rich granules (MRGs), organelles, heat-sensitive protein (HSPs), cellular debris, and heat-denatured protein (HDP) are provided in Figure S3. Under the 2.0 mg-Ti/L nano-$TiO_2$ treatment, *As* increased in cellular debris and HDP, whereas it decreased slightly in HSP. Under the 20.0 mg-Ti/L nano-$TiO_2$ treatment, *As* increased in the four fractions with the exception of HSP. HSP was the main binding site for nano-$TiO_2$ under both lower (2.0 mg-Ti/L) and higher (20.0 mg-Ti/L) concentrations.



DOI: 10.1021/acs.est.6b01215
Environ. Sci. Technol. 2016, 50, 9636−9643

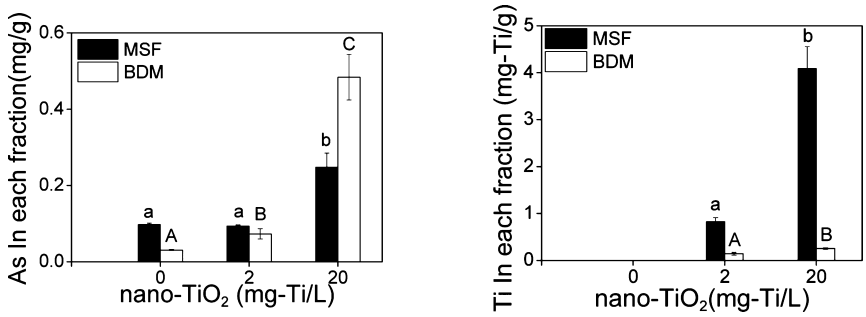


**Figure 5.** Subcellular distribution of arsenate and titanium in *Daphnia magna* after exposure to different nano-$TiO_2$ concentrations for 3 h. Mean ± standard deviations ($n$ = 3). Different letters indicate a statistically significant difference ($P$ < 0.05). MSF is the metal-sensitive fraction. BDM is biologically detoxified metal.

Metals associated with organelles and HSP could be viewed together as metal-sensitive fractions (MSF), while metals sequestered in HDP and MRG could be defined as biologically detoxified metals (BDM).[29,30] When exposed to low nano-$TiO_2$ concentrations (2.0 mg-Ti/L), *As* in MSF was not significantly different from that of the controls ($P$ > 0.05), whereas *As* in BDM was greater by a factor of almost 2.5 than the control (Figure 5). In contrast, *Ti* concentrations were higher in MSF than in BDM. When exposed to high nano-$TiO_2$ concentrations (20.0 mg-Ti/L), *As* in MSF increased by a factor of 2.5 compared to the control, but *As* in BDM increased by a far greater factor of 15.7 ($P$ < 0.05, $n$ = 3; Figure 5). At the same time, *Ti* concentrations significantly increased in MSF but only slightly increased in BDM ($P$ < 0.05, $n$ = 3). Compared to the control, subcellular *As* concentrations significantly increased in BDM, but subcellular *Ti* concentrations increased more in MSF. Therefore, we found significant differences in subcellular distribution of *As* and *Ti* in *D. magna*. Hence, a fraction of the introduced As(V) carried by nano-$TiO_2$ could dissociate and transport itself separately, which sorbed onto nano-$TiO_2$ before entering into *D. magna*.

It has generally been assumed that metals are first associated with the biologically inactive pool as the initial storage site, such as BDM.[30] Once this pool is saturated, metals are then channeled into biologically active pools, such as MSF.[30] Such spillover effects therefore cause direct biological response (or toxicity) in organisms, which are initially sublethal but eventually lethal. In turn, As(V) that accumulates in BDM does not produce toxic effects. Therefore, the decreased toxicity of As(V) at lower nano-$TiO_2$ concentrations results from unaffected *As* in MSF (compared to the control). Furthermore, As(V) (negatively charged) is most likely sorbed onto nano-$TiO_2$ via the formation of inner-sphere bidentate ligands and van der Waals forces.[53] This binding of As(V) in nano-$TiO_2$ could lead to a lower release within *D. magna*, subsequently further reducing its toxicity levels.

However, as total *As* accumulation increased with increasing nano-$TiO_2$ concentrations in *D. magna*, the As(V) released from nano-$TiO_2$ in *D. magna* reached a certain toxicity level, which may be lethal for *D. magna* survival. Under these circumstances, As(V) toxicity would subsequently increase. At the higher nano-$TiO_2$ concentration (20.0 mg-Ti/L), a greater amount of *As* was allocated in MSF compared to both the control and the lower nano-$TiO_2$ concentration (2.0 mg-Ti/L), which was greater by a factor of 2. Because some of the introduced As(V) carried by nano-$TiO_2$ could dissociate and transport separately, greater increases in *As* in MSF could dissociate from nano-$TiO_2$ during a free phase to individually play their own toxic roles in *D. magna* survival. The release of As(V) in MSF possibly overwhelms the ability of *D. magna* to detoxify itself, leading to an increase in its toxicity. Increased As(V) toxicity at higher nano-$TiO_2$ concentrations results from large increases in total *As* in MSF and its higher dissociation.

In summary, nano-$TiO_2$ as carriers significantly facilitated As(V) uptake by *D. magna*. Even though *As* accumulation increased with increasing nano-$TiO_2$ concentrations in *D. magna*, As(V) toxicity associated with nano-$TiO_2$ had a dual effect. Decreased toxicity of As(V) associated with nano-$TiO_2$ at lower concentrations resulted from unaffected *As* concentrations in MSF, for which As(V) ions were still adsorbed by nano-$TiO_2$. Moreover, some of the entered As(V) carried by nano-$TiO_2$ could desorb and transport separately, causing increased toxicity at higher nano-$TiO_2$ concentrations. Hence, this study could further aid in our understanding of the aquatic risks of As(V) associated with nano-$TiO_2$. As it is well recognized, nanoparticles possess dramatically different physicochemical properties from bulk counterparts. It is clearly necessary to evaluate potential distribution and corresponding internal processes of cocontaminants associated with other nanoparticles and even their bulk counterparts in aquatic environments during comprehensive risk assessments. Furthermore, the subcellular distribution method was defined in operational ways to separate subcellular fractions of contaminants in an organism, which will possibly cause the redistribution of contaminants. Despite that it had already been used to explain subcellular distribution and toxicity of contaminants as well as its levels of tolerance, this method should be applied prudently. Additionally, there are many *As* forms in the environment, but inorganic *As* (arsenite and arsenate) predominates. Arsenic accumulation is quite complex in aquatic organisms, involving *As* oxidation, reduction, methylation, and efflux as well as environmental factors.[33,54] Future studies should endeavor to understand how *As* metabolism is influenced by nano-$TiO_2$ in aquatic organisms.

## ■ ASSOCIATED CONTENT

### Supporting Information

The Supporting Information is available free of charge on the ACS Publications website at DOI: 10.1021/acs.est.6b01215.

Table S1 shows typical operational conditions for LA-ICP-MS analysis. Methods to measure *As* and nano-$TiO_2$ concentrations in daphnids are provided in Figure S1 to Figure S3 (PDF).



DOI: 10.1021/acs.est.6b01215
*Environ. Sci. Technol.* 2016, 50, 9636−9643

## AUTHOR INFORMATION


### Corresponding Authors

*Z. Luo. Telephone: +86 0592-6190545. Email: zxluoire@163.com.

*C. Yan. Email: czyan@iue.ac.cn.


### Notes

The authors declare no competing financial interest.

## ACKNOWLEDGMENTS

We thank the various anonymous reviewers for their helpful comments. We also thank Dr. Gang Li from the Institute of Urban Environment, CAS, for technical assistance with drawing LA-ICP-MS maps. This study was jointly funded by the National Nature Science Foundation of China (41271484, 41401552, and 41301346) and the Open Fund of the Fujian Provincial Key Laboratory of Resources and Environment Monitoring & Sustainable Management and Utilization (ZD1402).

## REFERENCES


(1) Hanumanthu, S. C. Emerging Discipline Nanotoxicology: Sources, Challenges and Strategies for Addressing Risk. *Int. J. Eng. Sci. Innovative Technol.* **2015**, *4* (5), 2319−5967.

(2) Gao, Y.; Yang, T.; Jin, J. Nanoparticle pollution and associated increasing potential risks on environment and human health: a case study of China. *Environ. Sci. Pollut. Res.* **2015**, *22*, 19297−19306.

(3) Grabowski, N.; Hillaireau, H.; Vergnaud, J.; Fattal, E. Evaluation of Lung Toxicity of Biodegradable Nanoparticles. In *Targeted Drug Delivery: Concepts and Design*; Springer: 2015; pp 689−732.

(4) Pachapur, V.; Brar, S. K.; Verma, M.; Surampalli, R. Y. Nano-Ecotoxicology of Natural and Engineered Nanomaterials for Animals and Humans. *Nanomaterials in the Environment*, 2015; pp 421−437; DOI: 10.1061/9780784414088.ch16.

(5) Abedin, F.; Anwar, M. R.; Asmatulu, R. Risk Assessments of Green Photo-active Nanomaterials. *Green Photo-active Nanomaterials: Sustainable Energy and Environment Remediation*, 2015; pp 364−384; DOI: 10.1039/9781782622642-00364.

(6) Ayati, A.; Ahmadpour, A.; Bamoharram, F. F.; Tanhaei, B.; Manttari, M.; Sillanpaa, M. A review on catalytic applications of Au/TiO2 nanoparticles in the removal of water pollutant. *Chemosphere* **2014**, *107*, 163−174.

(7) Jafari Kang, A.; Baghdadi, M.; Pardakhti, A. Removal of cadmium and lead from aqueous solutions by magnetic acid-treated activated carbon nanocomposite. *Desalin. Water Treat.* **2016**, *57*, 18782−18798.

(8) Handy, R. D.; Cornelis, G.; Fernandes, T.; Tsyusko, O.; Decho, A.; Sabo-Attwood, T.; Metcalfe, C.; Steevens, J. A.; Klaine, S. J.; Koelmans, A. A.; Horne, N. Ecotoxicity test methods for engineered nanomaterials: practical experiences and recommendations from the bench. *Environ. Toxicol. Chem.* **2012**, *31* (1), 15−31.

(9) Zhang, J.; Wages, M.; Cox, S. B.; Maul, J. D.; Li, Y.; Barnes, M.; Hope-Weeks, L.; Cobb, G. P. Effect of titanium dioxide nanomaterials and ultraviolet light coexposure on African clawed frogs (Xenopus laevis). *Environ. Toxicol. Chem.* **2012**, *31* (1), 176−183.

(10) Landsiedel, R.; Kapp, M. D.; Schulz, M.; Wiench, K.; Oesch, F. Genotoxicity investigations on nanomaterials: methods, preparation and characterization of test material, potential artifacts and limitations—many questions, some answers. *Mutat. Res., Rev. Mutat. Res.* **2009**, *681* (2), 241−258.

(11) Kimura, E.; Kawano, Y.; Todo, H.; Ikarashi, Y.; Sugibayashi, K. Measurement of skin permeation/penetration of nanoparticles for their safety evaluation. *Biol. Pharm. Bull.* **2012**, *35* (9), 1476−1486.

(12) Park, E.-J.; Yi, J.; Chung, K.-H.; Ryu, D.-Y.; Choi, J.; Park, K. Oxidative stress and apoptosis induced by titanium dioxide nanoparticles in cultured BEAS-2B cells. *Toxicol. Lett.* **2008**, *180* (3), 222−229.

(13) Bermudez, E.; Mangum, J. B.; Wong, B. A.; Asgharian, B.; Hext, P. M.; Warheit, D. B.; Everitt, J. I. Pulmonary responses of mice, rats, and hamsters to subchronic inhalation of ultrafine titanium dioxide particles. *Toxicol. Sci.* **2004**, *77* (2), 347−357.

(14) Federici, G.; Shaw, B. J.; Handy, R. D. Toxicity of titanium dioxide nanoparticles to rainbow trout (Oncorhynchus mykiss): Gill injury, oxidative stress, and other physiological effects. *Aquat. Toxicol.* **2007**, *84* (4), 415−430.

(15) Zhu, X.; Chang, Y.; Chen, Y. Toxicity and bioaccumulation of TiO 2 nanoparticle aggregates in Daphnia magna. *Chemosphere* **2010**, *78* (3), 209−215.

(16) Lovern, S. B.; Klaper, R. Daphnia magna mortality when exposed to titanium dioxide and fullerene (C60) nanoparticles. *Environ. Toxicol. Chem.* **2006**, *25* (4), 1132−1137.

(17) Heinlaan, M.; Ivask, A.; Blinova, I.; Dubourguier, H.-C.; Kahru, A. Toxicity of nanosized and bulk ZnO, CuO and TiO 2 to bacteria Vibrio fischeri and crustaceans Daphnia magna and Thamnocephalus platyurus. *Chemosphere* **2008**, *71* (7), 1308−1316.

(18) Diebold, U. The surface science of titanium dioxide. *Surf. Sci. Rep.* **2003**, *48* (5), 53−229.

(19) Dutta, P. K.; Ray, A. K.; Sharma, V. K.; Millero, F. J. Adsorption of arsenate and arsenite on titanium dioxide suspensions. *J. Colloid Interface Sci.* **2004**, *278* (2), 270−275.

(20) Liufu, S.; Xiao, H.; Li, Y. Adsorption of poly (acrylic acid) onto the surface of titanium dioxide and the colloidal stability of aqueous suspension. *J. Colloid Interface Sci.* **2005**, *281* (1), 155−163.

(21) Sun, H.; Zhang, X.; Niu, Q.; Chen, Y.; Crittenden, J. C. Enhanced accumulation of arsenate in carp in the presence of titanium dioxide nanoparticles. *Water, Air, Soil Pollut.* **2007**, *178* (1−4), 245−254.

(22) Zhang, X.; Sun, H.; Zhang, Z.; Niu, Q.; Chen, Y.; Crittenden, J. C. Enhanced bioaccumulation of cadmium in carp in the presence of titanium dioxide nanoparticles. *Chemosphere* **2007**, *67* (1), 160−166.

(23) Yang, W.-W.; Wang, Y.; Huang, B.; Wang, N.-X.; Wei, Z.-B.; Luo, J.; Miao, A.-J.; Yang, L.-Y. TiO2 nanoparticles act as a carrier of Cd bioaccumulation in the ciliate Tetrahymena thermophila. *Environ. Sci. Technol.* **2014**, *48* (13), 7568−7575.

(24) Caumette, G.; Koch, I.; Moriarty, M.; Reimer, K. J. Arsenic distribution and speciation in Daphnia pulex. *Sci. Total Environ.* **2012**, *432*, 243−250.

(25) Li, Y.; Yang, Y.; Jiao, S.; Wu, F.; Yang, J.; Xie, L.; Huang, C. In situ determination of hafnium isotopes from rutile using LA-MC-ICP-MS. *Sci. China: Earth Sci.* **2015**, *58* (12), 2134−2144.

(26) Melekestseva, I. Y.; Maslennikov, V. V.; Maslennikova, S. P.; Danyushevsky, L. V.; Large, R. R. Toxic and Valuable Elements in Fe-Rich and Cu-Zn-Rich Sulfides from the Semenov Hydrothermal Fields, MAR: a LA-ICP-MS Study. *Mar. Min. Resour.* **2015**, *3*, 1257−1260.

(27) Douglas, D. N.; O'Reilly, J.; O'Connor, C.; Sharp, B. L.; Goenaga-Infante, H. Quantitation of the Fe spatial distribution in biological tissue by online double isotope dilution analysis with LA-ICP-MS: a strategy for estimating measurement uncertainty. *J. Anal. At. Spectrom.* **2016**, *31*, 270−279.

(28) Fernandez, E. B.; Van Malderen, S. J. M.; Balcaen, L.; Resano, M.; Vanhaecke, F. Laser ablation−tandem ICP−mass spectrometry (LA-ICP-MS/MS) for direct Sr isotopic analysis of solid samples with high Rb/Sr ratio. *J. Anal. At. Spectrom.* **2016**, *31*, 464−472.

(29) Wang, W. X.; Guan, R. Subcellular distribution of zinc in Daphnia magna and implication for toxicity. *Environ. Toxicol. Chem.* **2010**, *29* (8), 1841−1848.

(30) Wallace, W. G.; Lee, B.-G.; Luoma, S. N. Subcellular compartmentalization of Cd and Zn in two bivalves. I. Significance of metal-sensitive fractions (MSF) and biologically detoxified metal (BDM). *Mar. Ecol.: Prog. Ser.* **2003**, *249*, 183−197.

(31) Sanders, B. M.; Jenkins, K. D.; Sunda, W. G.; Costlow, J. D. Free cupric ion activity in seawater: effects on metallothionein and growth in crab larvae. *Science* **1983**, *222* (4619), 53−55.




DOI: 10.1021/acs.est.6b01215
*Environ. Sci. Technol.* 2016, 50, 9636−9643

(32) Klerks, P.; Bartholomew, P. Cadmium accumulation and detoxification in a Cd-resistant population of the oligochaete Limnodrilus hoffmeisteri. *Aquat. Toxicol.* **1991**, *19* (2), 97−112.
(33) Wang, Z. H.; Luo, Z. X.; Yan, C. Z.; Che, F. F.; Yan, Y. M. Arsenic uptake and depuration kinetics in Microcystis aeruginosa under different phosphate regimes. *J. Hazard. Mater.* **2014**, *276*, 393−399.
(34) *Test No. 202: Daphnia sp. Acute Immobilisation Test*; OECD, 2004; DOI: 10.1787/9789264069947-en.
(35) Tan, C.; Fan, W.-H.; Wang, W.-X. Role of titanium dioxide nanoparticles in the elevated uptake and retention of cadmium and zinc in Daphnia magna. *Environ. Sci. Technol.* **2012**, *46* (1), 469−476.
(36) Adam, N.; Schmitt, C.; Galceran, J.; Companys, E.; Vakurov, A.; Wallace, R.; Knapen, D.; Blust, R. The chronic toxicity of ZnO nanoparticles and ZnCl2 to Daphnia magna and the use of different methods to assess nanoparticle aggregation and dissolution. *Nanotoxicology* **2014**, *8* (7), 709−717.
(37) Ulrich, T.; Guenther, D.; Heinrich, C. Gold concentrations of magmatic brines and the metal budget of porphyry copper deposits. *Nature* **1999**, *399* (6737), 676−679.
(38) Eggins, S.; Kinsley, L.; Shelley, J. Deposition and element fractionation processes during atmospheric pressure laser sampling for analysis by ICP-MS. *Appl. Surf. Sci.* **1998**, *127*, 278−286.
(39) Hartmann, N. B.; Von der Kammer, F.; Hofmann, T.; Baalousha, M.; Ottofuelling, S.; Baun, A. Algal testing of titanium dioxide nanoparticles-Testing considerations, inhibitory effects and modification of cadmium bioavailability. *Toxicology* **2010**, *269* (2−3), 190−197.
(40) Rosenfeldt, R. R.; Seitz, F.; Schulz, R.; Bundschuh, M. Heavy Metal Uptake and Toxicity in the Presence of Titanium Dioxide Nanoparticles: A Factorial Approach Using Daphnia magna. *Environ. Sci. Technol.* **2014**, *48* (12), 6965−6972.
(41) Spehar, R. L.; Fiandt, J. T.; Anderson, R. L.; DeFoe, D. L. Comparative toxicity of arsenic compounds and their accumulation in invertebrates and fish. *Arch. Environ. Contam. Toxicol.* **1980**, *9* (1), 53−63.
(42) Seitz, F.; Bundschuh, M.; Rosenfeldt, R. R.; Schulz, R. Nanoparticle toxicity in Daphnia magna reproduction studies: The importance of test design. *Aquat. Toxicol.* **2013**, *126*, 163−168.
(43) Rosenfeldt, R. R.; Seitz, F.; Schulz, R.; Bundschuh, M. Heavy Metal Uptake and Toxicity in the Presence of Titanium Dioxide Nanoparticles: A Factorial Approach Using Daphnia magna. *Environ. Sci. Technol.* **2014**, *48* (12), 6965−6972.
(44) Wang, D.; Hu, J.; Irons, D. R.; Wang, J. Synergistic toxic effect of nano-TiO 2 and As (V) on Ceriodaphnia dubia. *Sci. Total Environ.* **2011**, *409* (7), 1351−1356.
(45) Geller, W.; Müller, H. The filtration apparatus of Cladocera: filter mesh-sizes and their implications on food selectivity. *Oecologia* **1981**, *49* (3), 316−321.
(46) Gophen, M.; Geller, W. Filter mesh size and food particle uptake by Daphnia. *Oecologia* **1984**, *64* (3), 408−412.
(47) Hartmann, H. J.; Kunkel, D. D. Mechanisms of food selection in Daphnia. *Hydrobiologia* **1991**, *225* (1), 129−154.
(48) Fan, W.; Cui, M.; Liu, H.; Wang, C.; Shi, Z.; Tan, C.; Yang, X. Nano-TiO 2 enhances the toxicity of copper in natural water to Daphnia magna. *Environ. Pollut.* **2011**, *159* (3), 729−734.
(49) Lee Rodgers, J.; Nicewander, W. A. Thirteen ways to look at the correlation coefficient. *Am. Stat.* **1988**, *42* (1), 59−66.
(50) Wang, W. X.; Guo, L. D. Influences of natural colloids on metal bioavailability to two marine bivalves. *Environ. Sci. Technol.* **2000**, *34* (21), 4571−4576.
(51) Tan, C.; Fan, W. H.; Wang, W. X. Role of Titanium Dioxide Nanoparticles in the Elevated Uptake and Retention of Cadmium and Zinc in Daphnia magna. *Environ. Sci. Technol.* **2012**, *46* (1), 469−76.
(52) Mohan, D.; Pittman, C. U. Arsenic removal from water/wastewater using adsorbents - A critical review. *J. Hazard. Mater.* **2007**, *142* (1−2), 1−53.
(53) Nabi, D.; Aslam, I.; Qazi, I. A. Evaluation of the adsorption potential of titanium dioxide nanoparticles for arsenic removal. *J. Environ. Sci.* **2009**, *21* (3), 402−408.
(54) Wang, Y.; Wang, S.; Xu, P. P.; Liu, C.; Liu, M. S.; Wang, Y. L.; Wang, C. H.; Zhang, C. H.; Ge, Y. Review of arsenic speciation, toxicity and metabolism in microalgae. *Rev. Environ. Sci. Bio/Technol.* **2015**, *14* (3), 427−451.


DOI: 10.1021/acs.est.6b01215
*Environ. Sci. Technol.* 2016, 50, 9636−9643